



Full Length Article

Isolation and Evaluation of Bioactive Compounds from *Rheum emodi* and their Anti-Inflammatory and Anticancer Properties

Sang Koo Park¹ and Seon Young Im^{2*}

¹Food Safety Management Division, Seoul Regional Korea Food and Drug Administration, Seoul 07978, Korea

²Department of Crop Science and Biotechnology, Dankook University, Cheonan 31119, Korea

*For correspondence: sy_im@dankook.ac.kr

Received 24 December 2020; Accepted 18 February 2021; Published 10 May 2021

Abstract

Rheum emodi Wall. ex Meissn is a popular medicinal herb having wide application in traditional medicine for treating of several diseases. The present study was aimed to identify and isolate phytochemicals present in ethyl acetate extract fraction of *R. emodi* and to evaluate the anticancer and anti-inflammatory activities of water/organic solvent fractions and isolated compounds of *R. emodi* rhizome extracts. Based on the structure, flavonoid compound *i.e.*, Myricitrin (sym. Myricetin 3-rhamnoside), myricetin 3-galloylrhamnoside and myricetin were identified to be present in ethyl acetate extract. The molecular weight of compound 1 cannot be identified; while compound 5 remained unknown as there was not enough evidence to propose its structure. The isolated compounds and different solvent fractions were tested for their anticancer and anti-inflammatory activities. Among Myricetins derivatives, particularly unknown compounds significantly induced the apoptosis and restrained the proliferation of cancer cell lines (A549 and MCF-7) and inhibited the LPS induced NO production (pro-inflammatory mediator), IL-6 activity, IL-1 β and TNF- α (cytokines) activity in RAW 264.7 macrophages in a dose dependent manner and was effective even at lower concentration (50 μ g/mL). Similarly, the higher concentration of aqueous and solvent fractions exhibited strong cytotoxic and anti-inflammatory activities. However, water and dichloromethane fractions were most effective in inhibiting the anticancer activities in A549 and MCF-7 cancer cell lines, respectively. At lower concentration (50 and 100 μ g/mL), highest inhibition activity for NO, IL-6 and IL-1 β was noted with ethyl acetate fractions and n-Hexane fractions; while water and n-Butanol (fractions) strongly inhibited the TNF- α activity at lower (100 μ g/mL) and high (200 μ g/mL) concentration, respectively. In conclusion, the isolated compounds from *R. emodi* rhizome extracts and its rhizome solvent fractions exhibit strong anti-cancer and anti-inflammatory activities and can be used to develop chemotherapeutics and anti-inflammation drugs. © 2021 Friends Science Publishers

Keywords: Flavonoids; Chemotherapy; Medicinal herb; Bioactive compounds; Macrophages

Introduction

Inflammation is a defense response of body against injury, pathological infection, noxious stimuli or trauma (Choi *et al.* 2012). Intense inflammation is often associated with several diseases such as diabetes, arthritis, Alzheimer's and cancer (Pereira and Alvarez-Leite 2014; Torres-Rodríguez *et al.* 2016; Qian 2017). In response of inflammation macrophages are activated by endotoxin like lipopolysaccharide (LPS). These LPS activated macrophage cells excrete several pro-inflammatory cytokines (tumor necrosis factor- α (TNF- α); interleukin-1 β (IL-1 β); interleukin-6 (IL-6) and mediators (*e.g.*, free radicals) such as nitric oxide (NO) (Li *et al.* 2014). Unregulated of excessive production of these mediators involved in arbitrating or exacerbating several diseases such as chronic pulmonary inflammatory disease,

arthritis, osteoarthritis, ulcerative colitis and carcinogenesis (Choi *et al.* 2014).

Cancer (severe metabolic disorder) is one of the major causes of human deaths globally (Iqbal *et al.* 2017); involves uncontrolled normal cells proliferation caused by genetic instabilities and alterations, which lead to malignant cells generation and metastasis initiation or tissue invasion (Krishnamurthi 2007). At present many therapies for cancer treatment include surgery, chemotherapy and radiotherapy have proved effective in saving lives of numerous cancer patients. Nevertheless, recurrence and severe side effects make these treatments partially effective, pressing the demand for treatments with low toxicity and minimal side effects. Plant derived chemicals compared to chemotherapy drugs are high target specific with low toxicity and can be used to unravel anticancer chemical agents (Cragg and Newman 2007). *Rheum* (*Rheum emodi* Wall. ex Meissn) is

an endemic, perennial, medicinal herb, commonly known as Himalayan Rhubarb; distributed in the Himalayas (subtropical and temperate regions), is widely used as traditional medicine against several diseases (Rokaya *et al.* 2012). The *R. emodi* contain several bioactive compounds such as anthraquinones, anthocyanins, flavonoids, stilbenes and desoxyrhapontigenin (Gao *et al.* 2011) and is known for its strong anti-inflammatory, anticancer, anti-oxidative and antimutagenic effects (Li *et al.* 2008). Among these phytochemicals, flavonoids (cannot synthesized by human and animal) is very important class of compounds which is essential constituent of animal and human diet and possess a therapeutic potential against cancer and inflammation (Raffa *et al.* 2017).

Few studies have reported that aqueous and methanolic extracts of *R. emodi* found to possess several anticancer (Rajkumar *et al.* 2011) and anti-inflammatory metabolites (Kounsar and Afzal 2010). However, there is very limited information on the relative efficacy of different organic solvent extracts of *R. emodi* on the anticancer and anti-inflammatory activities. Moreover, the isolation of flavonoids and their anti-inflammatory and anticancer activities in *R. emodi* is not well characterized. Therefore, the present study was carried out to evaluate the *in vitro* anticancer and anti-inflammatory activities of the rhizome extracts fractions of *R. emodi* using different organic solvents and to isolate and identify the flavonoid compounds from ethyl acetate extracts and to evaluate the anti-inflammatory and anti-cancer potential of isolated compounds.

Materials and Methods

Plant material

R. emodi was collected from Langtang at an altitude of 3,500 m in Nepal. The plant was identified using standard references and authenticated by a botanist. The voucher specimen was deposited in the gene bank of Dankook University.

Chemicals

LPS (Lipopolysaccharide), DMSO and Griess' reagent for nitrite were procured from Sigma Chemical Co. (St. Louis, MO, USA). The ELISA kit (IL-6, IL-1 β , TNF- α) was purchased from BD Biosciences (USA). BHT, L-ascorbic acid, Rutin, Gallic acid, Trizma base, NADH, MTT (3-(4,5-dimethylthiazol-2-yl)-2,5-diphenyl tetrazolium bromide), PMS (phenazine methosulphate), NBT (nitroblue tetrazolium), TBA (thiobarbituric acid), TCA (trichloroacetic acid), Trolox (6-hydroxy-2,5,7,8-tetramethylchroman-2-carboxylic acid), ammonium thiocyanate and Foli-Ciocalteu's phenol reagent were procured from Sigma Chemical Co. (St. Louis, MO, USA). The HPLC reagents were water, methanol and acetonitrile

from J. T. Baker (USA). All other chemicals and solvents were commercial analytical grade.

Extraction and solvent fraction of *R. emodi*

The air-dried *R. emodi* rhizomes were crushed in a grinder for 2 min, the process was stopped for 15 s intervals to prevent samples from heating. The *R. emodi* samples (800 g) were extracted with 70% EtOH under reflux (3 \times 2.5 L, 2 h each time), followed by filtration through filter paper (Whatman No. 2). Later, rotary vacuum-evaporator at 50°C under reduced pressure was used to evaporate the solvent of combined extract; while freeze drying helped in removal of remaining water. The crude extract obtained by concentrating the EtOH extract under vacuum was suspended in water and later sequentially extracted with *n*-hexane (room temperature, 2 \times 1 L) followed by dichloromethane (2 \times 1 L), EtOAc (2 \times 1 L), *n*-BuOH (2 \times 1 L) and water, in order (Fig. S1). The solvents from each step were removed by evaporation and then freeze-dried. The dried solvent fractions were stored below -18°C in deep freezer.

Isolation and identification of bioactive compound

The method of Lin and Harnly (2007) was followed for identification of phenolic compounds. This protocol obtains mass spectrometric data as negative and positive ionization mode at high (250 V) and low (70–100 V) and high excitation energy. The molecular ions are obtained from the negative ionization with low excitation; whereas high energy liberates fragments which show cinnamoyl quinic acids (mono-, di-, or trihydroxy) by successive loss of hydroxy cinnamoyls. However, UV and MS data and retention time comparison from sample peaks with standards helps in positive compound identification. The method has accumulated a large database of phenolic compounds collected from routine profiling and analysis of standards and is being used for their presence and identification in new plant sources (Lin and Harnly 2007).

Isolation and identification of antioxidant compound by LC-DAD-ESI/MS

The compounds present in *R. emodi* fractions were isolated using Micromass ZQ MS and an Alliance e2695 HPLC system (Waters Co., Milford, M.A., USA) equipped with a 2998 photodiode array detector in addition to a YMC PACK ODS-AM reversed-phase column (4.6 x 250 nm I.D., 5 μ m; YMC Co. Ltd., Japan). The analysis was conducted at 190–600 nm (the characteristic wavelength of 254, 350 nm) detection wavelengths with 1 mL/min flow rate and oven temperature of 30°C. Trifluoroacetic acid (0.1%) in water (phase A) and acetonitrile (phase B) were used as mobile phases. The pretreated samples were analyzed by using a gradient of 10 to 30% of phase B over

25-min period; 30% of phase B for five minutes; gradient of 30 to 10% of phase B for three minutes and then final wash with 10% phase B for seven minutes. The electrospray ionization source was used to run the MS analysis in a positive ionization mode and MS parameters were set to 30 V (cone voltage), 120°C (source temperature), 350°C (desolvation temperature) and 500 L/h (desolvation N₂ gas flow). The molecular weight range was 100–1200 *m/z* in the full scan mode.

Preparative antioxidant compounds by LC/MS system

The analysis protocol was similar to isolation and identification of antioxidant compound by LC-DAD-ESI/MS. In addition, the fractionation parameters were set to maximum fractions and tubes per injection of 78, solvent front delay of 60 s, spilt/collector delay of 10 s and maximum fraction width of 60 s. The Ethyl acetate fraction from *R. emodi* with concentration of 50,000 ppm was used for 500 μ L per injection. In two step purification, the fractionation parameters were different with the first step as follow: maximum tubes per injection of 114, maximum fraction width of 30 s. The Ethyl acetate fraction from *R. emodi* with concentration of 50,000 ppm was used for 200 μ L per injection.

The fractions collected in tubes were directly analyzed without any additional liquid handling. Proper wash of the injection was found to be most important procedure for the proper purity check of collected fractions after preparative purification. Before analytical runs of each series, needle was washed and blank injection with MeOH 70% was used.

Peak purity of collected fractions with their main component was evaluated using relative peak area in mass chromatograms, thus assuming comparable response factor for the impurities and the major component.

Chemical structures of bio active compounds from *R. emodi*

ChemDraw Ultra 8.0 software (CambridgeSoft, USA) was used for drawing the chemical structures of compounds.

Anti-inflammatory activity assays

Cell culture: The RAW 264.7 (mouse macrophage cell line) obtained from Korean cell line bank, Seoul, Korea was grown in Dulbecco's modified Eagle's medium having fetal bovine serum (10%). The macrophages were kept at 37°C in humidified atmosphere having 5% CO₂. For the experiment, RAW 264.7 cells were subculture for every 2~3 days.

Cell viability

To evaluate the effect of extracts on the cell viability, cytotoxicity assay was performed. The RAW 264.7 macrophage cell was seeded onto 96-well plate at 10⁴ ~10⁵

cell/well then cultured in 5% CO₂ incubator at 37°C for 24 h. The cells were treated with final concentration of 10, 25 and 50 μ g/mL of the extracts. The cells were incubated for further 24 h. The medium was exchanged with 180 μ L fresh medium contained 20 μ L of 0.5 mg/mL MTT solution in each well. The absorbance for isolated compounds and solvent extract fractions was measured at 450 and 570 nm respectively using microplate reader after 1~4 h.

NO inhibition activity

The RAW 264.7 macrophage cell was seeded onto 96-well plate at 10⁴ ~10⁵ cell/well then cultured in 5% CO₂ incubator at 37°C for 24 h. The cells were incubated in 1 μ g/mL of medium containing LPS (Sigma Co.) and final concentration of 10, 25 and 50 μ g/mL each sample. The cells were incubated for further 24 h. The NO inhibition activity was analyzed by Griess assay. The Griess' reagent (0.1% naphthylethylenediamine and 1% sulfanilamide in 5% H₃PO₄ solution) was added to each of the supernatant from the cells treated with samples. Sodium nitrite was used as positive control. No contents were read at 540 nm against a standard sodium nitrite curve.

IL-6, IL-1 β , and TNF- α inhibition activity

The RAW 264.7 macrophage cell was seeded onto 96-well plate at 10⁴ ~10⁵ cell/well then, cultured in 5% CO₂ incubator at 37°C for 24 h. The cell were incubated in a medium containing LPS (Sigma Co.) 1 μ g/mL and final concentration 10, 25 and 50 μ g/mL each samples. The cells were incubated for an additional 24 h. The IL-6, IL-1 β , TNF- α inhibition activity was analyzed by commercially available ELISA kit (BD OptEIA™ set Mouse IL-6, IL-1 β , TNF- α). The assay was performed as described by the manufacturer's recommendations.

Anticancer activity assays

Cell culture: Cytotoxicity of the extracts were determined in MCF7 (human breast carcinoma) and A549 (lung carcinoma) from Korean cell line bank, Seoul, Korea, HGF (Human gingival fibroblast) form Department of Dentistry from Dankook University. The cells were kept at 37°C in humidified atmosphere containing 5% CO₂; grown in minimum essential medium and RPMI 1640 medium with fetal bovine serum (10%). The cells were subcultured every 2~3 days.

Cytotoxicity assay

To evaluate effects of extracts on the cell viability, a cytotoxicity assay was performed. The cancer cells (MCF7, A549) were seeded onto 96-well plate at 10⁴ ~10⁵ cell/well then, cultured in 5% CO₂ incubator at 37°C for 24 h and cells were treated with final concentration 20, 50, 100, 200

mg/mL of extracts. The cells were incubated for further 24 h and medium was changed with 200 μ L fresh medium contained 10 μ L of CCK-8 (Dojindo, Japan) solution in each well. The absorbance was measured at 570 nm using microplate reader after further 1~4 h.

Calculation of half maximal inhibitory concentration (IC₅₀)

IC₅₀ value, the sample concentration required to scavenge 50% of the free radicals, were calculated using the percent scavenging activities of the different sample concentrations.

Statistical analysis

General analysis: The experimental data were analyzed by SPSS (version 12.0 for windows XP, SPSS Inc.) using one and two-way analysis of variance, while Duncan's multiple range test was performed for mean separation ($P < 0.05$).

Multivariate analysis (partial least squares of discriminant analysis (PLS-DA))

The data matrix was developed by arranging and normalizing all the qualitative and quantitative information, which is used for multivariate statistical analysis as log₁₀-transformed data. SIMCA-P 11.0 software (Umetrics, Umea, Sweden) was used for performing PLS-DA models.

Results

Identification of antioxidant compounds

Five peaks were obtained from ethyl acetate fraction of *R. emodi* based on their retention time and detection wavelength of 190–600 nm by LC-DAD-ESI/MS. These peaks were separated into compound 1 (Rt = 5.30 min), compound 2 (Rt = 17.30 min), compound 3 (Rt = 23.30 min), compound 4 (Rt = 24.30 min) and compound 5 (Rt = 28.30 min) using an YMC PACK ODS-AM reversed-phase column (4.6 x 250 nm I.D., 5 μ m) and narrower range of solvent gradient (Fig. 1).

Compound 1 was identified based on the comparison of retention times, numerous literature sources and mass spectra data of the samples. Retention time of the peak was observed at 4.533 min, revealed a solvent peak. It was not possible to detect the mass even when the LC-DAD-ESI/MS experiment was performed. Likewise, compound 2 was identified using literature sources and mass spectra data of the samples as Myricetin 3-O-rhamnoside (Myricitrin) at the retention time of 17.80 min through comparison of the retention times, ion was revealed at 464 m/z with a molecular formula $C_{21}H_{20}O_{12}$ (Fig. 2). Compound 3 was identified as Myricetin 3-galloylrhamnoside at the retention time at 23.82 min, ion was revealed at 617 m/z with a molecular formula of $C_{28}H_{24}O_{16}$ (Fig. 3). Remarkably, this compound was found in this plant for the first time.

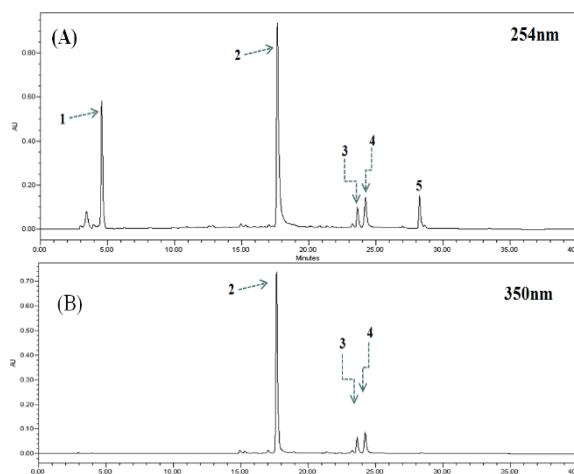


Fig. 1: LC chromatogram (254 nm and 350 nm) of ethyl acetate fraction from *R. emodi*

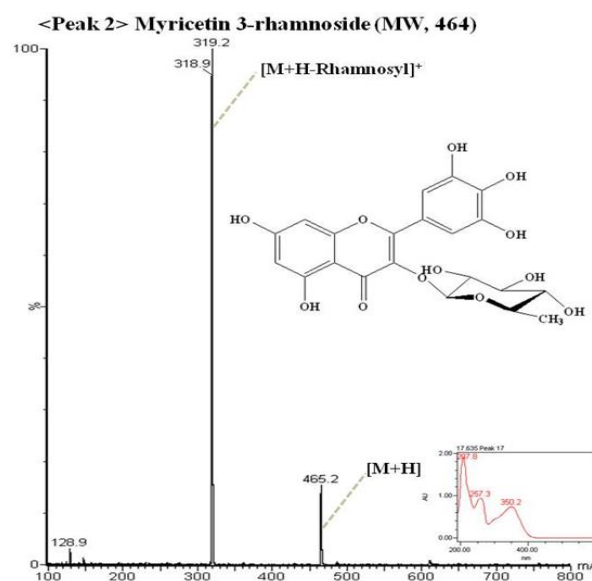


Fig. 2: Structure and MS spectra about compound 1 isolated from *R. emodi* by LC-DAD-ESI/MS

Compound 4 was identified as Myricetin (Fig. 4), at the retention time of 24.37 min, ion was revealed at 319 m/z with a molecular formula of $C_{15}H_{10}O_8$. Accordingly, compound 5 was identified as unknown (Fig. 5) at retention time of 28.465 min, ion was revealed at around 520 m/z . It was not possible to elucidate a structure even when the LC-DAD-ESI/MS experiment was performed. There was not enough evidence to propose the structure of the compound. Positive ion electrospray analysis, total ionic current profile and reconstructed ion chromatograms of compound 2–5 (Fig. 2–5) identified the Myricetin derivatives through comparison of retention times and m/z values in the total ion current chromatogram from the data gotten from the literature. The ion chromatograms were reconstructed for each value of m/z observed for the standard compounds 2

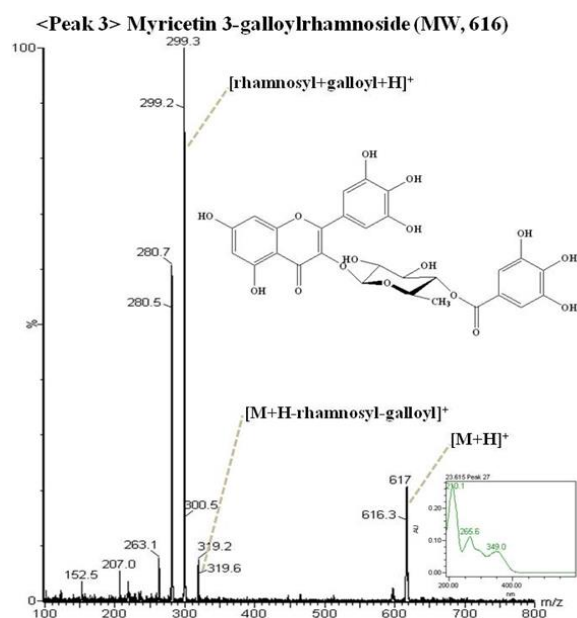


Fig. 3: Structure and MS spectra about compound 2 isolated from *R. emodi* by LC-DAD-ESI/MS

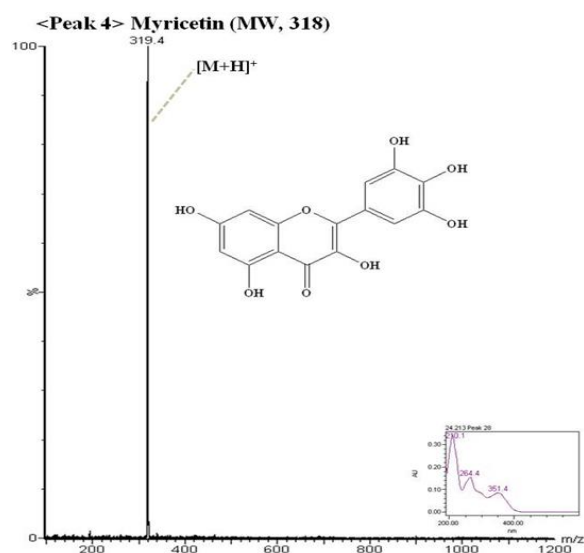


Fig. 4: Structure and MS spectra about compound 3 isolated from *R. emodi* by LC-DAD-ESI/MS

(319 and 464 m/z), 3 (280, 299, 319, 465 and 617 m/z), and 4 (319 m/z) to advance the separation and the recognition of single compounds. LC-DAD-ESI/MS analysis of compound 2 discovered the presence of myricetin related compounds. Specifically, peaks at 464 m/z were observed and the reconstructed ion chromatograms revealed one peak; the value of the mass of the pseudo molecular ion, the retention and the presence in this fraction suggested that these compounds were Rhamnoside (145 m/z). The presences of the fragment ion at 463.0853 m/z indicate the loss of a galloyl moiety and the presence of myricetin rhamnoside

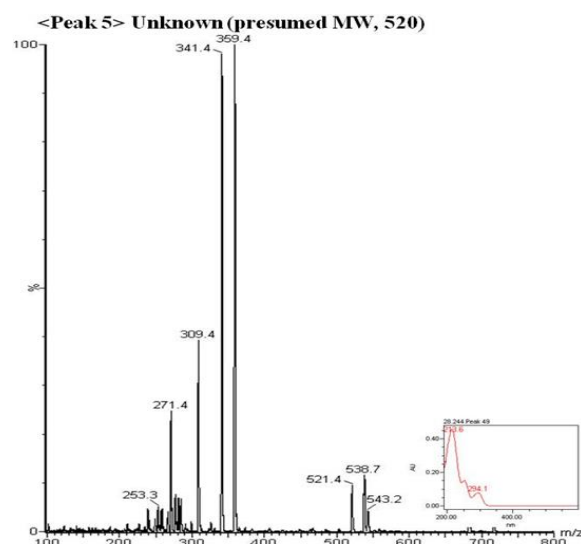


Fig. 5: Structure and MS spectra about compound 4 isolated from *R. emodi* by LC-DAD-ESI/MS

(Amani *et al.* 2014). The ion at 464, which corresponds to the myricetin (319 m/z) and rhamnoside (145 m/z), confirmed that this compound had the natural of Myricetin 3-O-rhamnoside (Myricitrin).

The LC-DAD-ESI/MS spectrum of compound 3 gave base peak of the $[M+H]^+$ ion at 617 m/z and molecular weight 616. The ion at 617 m/z , which corresponds to the myricetin (m/z 464) and gallic acid (m/z 152), which eluted at 14.90 min and showed 615.0988 m/z , it was confirmed that this compound was characterized as Myricetin 3-O-galloylrhamnoside according to the MS and MS/MS data and the literature. LC-DAD-ESI/MS analysis of compound 3 revealed the presence of other compounds related to myricetin. Specifically, peaks at 319 m/z were identified as myricetin. The LC-DAD-ESI/MS spectrum of compound 3 gave base peak of the $[M+H]^+$ ion at 319 m/z and molecular weight of 317. In addition, another fragment was presented at 280 m/z , which corresponds to the consequent loss of water molecule. Finally, the ion at 299 m/z , which corresponds to the subsequent loss of a rhamnoside (145 m/z) and gallic acid (152 m/z), it was confirmed that this compound was the basic structure.

Anticancer activities of *R. emodi*

Cytotoxic activity of isolated compounds on A549 and MCF-7 cell: The cytotoxic activity on A548 and MCF-7 were performed to estimate the anticancer activity potential of isolated compounds. Doxorubicin was used as a positive control. The IC_{50} (concentration needed for inhibition of 50% radical-scavenging effect) was verified from the results of a series of concentration tested. Lower IC_{50} value corresponds to a greater scavenging activity. The cytotoxic activity on A549 cell lines varied from IC_{50} 56.15 to 67.49 $\mu g/mL$ (Table 1). The IC_{50} values of the cytotoxicity

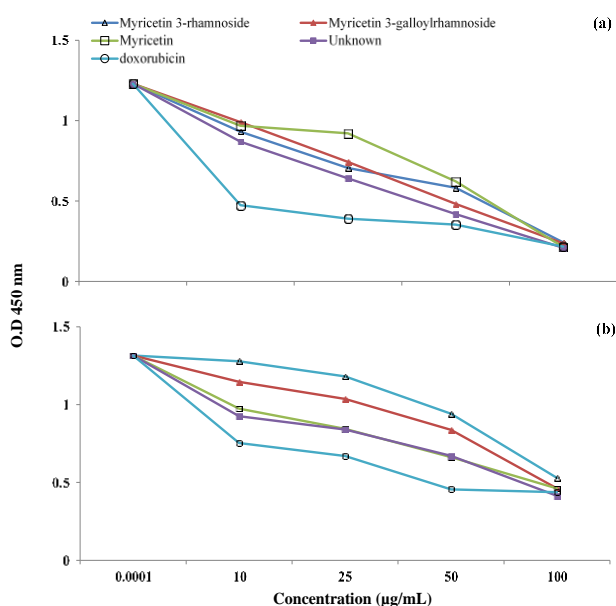
Table 1: Comparison of anticancer activity of antioxidant compounds from *R. emodi* in A549 and MCF-7 cells

Cell Lines	Fraction	IC ₅₀ (μg/mL)
A549	Myricetin 3-O-rhamnoside	64.04 ± 9.82 ^c
	Myricetin 3-O-galloylrhamnoside	62.21 ± 6.07 ^c
	Myricetin	67.49 ± 8.63 ^c
	Unknown	56.15 ± 9.37 ^b
	Doxorubicin*	41.68 ± 5.79 ^a
MCF-7	Myricetin 3-O-rhamnoside	104.76 ± 11.8 ^d
	Myricetin 3-O-galloylrhamnoside	93.35 ± 9.09 ^c
	Myricetin	84.35 ± 8.08 ^b
	Unknown	80.49 ± 8.39 ^b
	Doxorubicin*	70.17 ± 4.70 ^a

Each value represents means ± SD (n = 3)

a-d Values within a column followed by different letters are significant different ($P < 0.05$)

* Compound used as a positive control

**Fig. 6:** Cytotoxic activity of isolated compounds from *R. emodi* fractions on (a) A549 and (b) MCF-7 cancer cell lines

activities on A549 cells can be ranked as unknown (56.15 μg/mL) > myricetin 3-galloylrhamnoside (62.21 μg/mL) > Myricetin 3-rhamnoside (64.04 μg/mL) > Myricetin (67.49 μg/mL) (Table 1). All the compounds exhibited an excellent cytotoxicity activity. However, their IC₅₀ values were greater than that of Doxorubicin (41.68 μg/mL). Unknown compound showed very strong anticancer activity against A549 cells, with an IC₅₀ of 56.15 μg/mL. The cytotoxicity activity on A549 cell lines by concentration from compounds were expressed in a dose-dependent manner (Fig. 6a). The decrease in absorbance at high dose could be justified by cytotoxicity exhibited by the fractions.

The cytotoxic activity on MCF-7 cell lines varied from IC₅₀ of 80.49 to 104.76 μg/mL. The IC₅₀ values of the cytotoxicity activities on MCF-7 cells can be ranked as unknown (80.49 μg/mL) > myricetin (84.35 μg/mL) > Myricetin 3-galloylrhamnoside (93.35 μg/mL) > Myricetin

3-rhamnoside (104.76 μg/mL) (Table 1). Their IC₅₀ values were smaller than that of Doxorubicin (70.17 μg/mL). Unknown showed very strong anticancer activity against A549 and MCF-7 cells. The cytotoxic activities on MCF-7 cell lines by different concentration of compounds were expressed in the dose-dependent (Fig. 6b).

Cytotoxic activity of solvent extract fractions of *R. emodi* on A549 and MCF-7 cells

The *R. emodi* fractions significantly differed for cytotoxic activity on A549 cells. The IC₅₀ values of *R. emodi* fractions on A549 cell lines and Doxorubicin (positive controls) varied from 74.9 to 128.5 μg/mL (Table 2). The aqueous fraction exhibited the highest cytotoxic activity on A549 cell lines (74.9 μg/mL) followed by dichloromethane (93.6 μg/mL) > *n*-butanol (104.0 μg/mL) > *n*-hexane (106.14 μg/mL) > ethyl acetate (128.5 μg/mL) fractions.

The cytotoxicity activity of *R. emodi* fractions on A549 cell lines increased in the dose-dependent manner. In this regard, the water fraction of *R. emodi* inhibited A549 cell lines growth at 20, 50 and 100 μg/mL while *n*-Hexane showed highest cytotoxicity at 200 μg/mL on A549 cell lines (Fig. S3a).

The cytotoxic activity of *R. emodi* fractions significantly differed against MCF-7 cells. All fractions exhibited lower cytotoxic activity than Doxorubicin (control) (IC₅₀ 50.82 μg/mL) (Table 2). The cytotoxic activity on MCF-7 cell lines varied from IC₅₀ 114.72 to 139.36 μg/mL. However, among the tested fractions highest cytotoxic activity was observed for dichloromethane (114.72 μg/mL) > *n*-hexane (116.34 μg/mL) > water (122.6 μg/mL) > *n*-butanol (124.24 μg/mL) > ethyl acetate (139.36 μg/mL) (Table 2). The concentration of fractions on cytotoxicity activity against MCF-7 showed a linear rise with increase in fractions concentration (Fig. S3b). However, the dichloromethane fraction showed higher cytotoxic activity at all concentration than other fractions (Fig. S3a, b).

In vitro cytotoxicity of *R. emodi* fractions on A549 and MCF-7 cells

The *In vitro* study revealed that treatment with 50 mg/mL, 100 mg/mL and 200 mg/mL fractions dramatically induced black spot in a dose-dependent manner in A549 cells. The viability of A549 cells showed a significant decrease even at high concentration of *n*-Hexane fraction. The destruction of A549 cells was concentrated at 50 mg/mL in *n*-Hexane fraction. The water fraction was found to have the highest cytotoxic activity on A549 cell lines as visible from the destructed nucleus and nuclear compartment at 100 mg/mL of water fraction (Table 2; Fig. 7).

Treatment of MCF-7 cells with higher concentrations (50, 100 and 200 mg/mL) of *R. emodi* fractions induced the apoptosis. In this regard, *n*-Hexane fraction showed a significant inhibition of morphologic changes in MCF-7 cell.

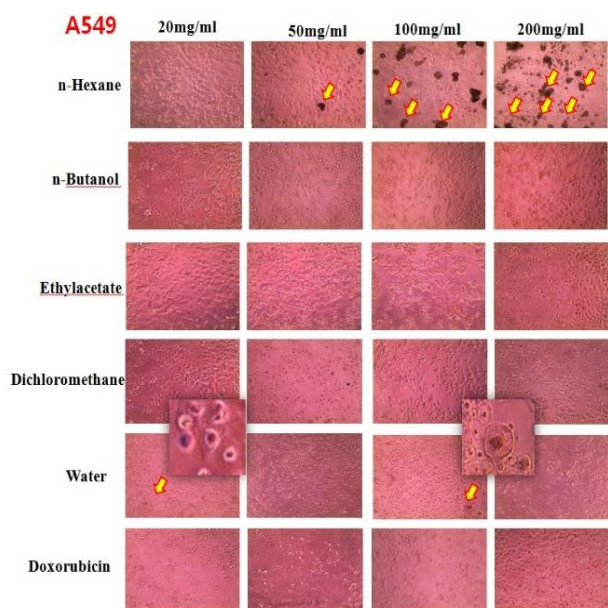


Fig. 7: Cytotoxic activity on A549 cell lines by different concentration of *R. emodi* compound

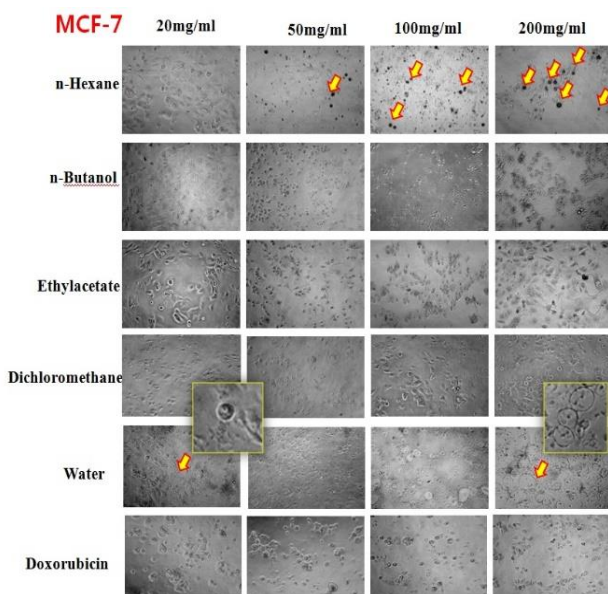


Fig. 8: The Cytotoxic activity of different *R. emodi* fractions on MCF-7 cell lines with different concentration

The data suggest that apoptosis of MCF-7 cancer cells was induced in dose-dependent manner, and these morphologic changes appeared with 50 mg/mL treatment (Fig. 8).

Anti-inflammatory activities of compounds isolated from *R. emodi*

NO inhibition activity: The NO production in the medium of RAW 264.7 cells cultured with LPS was measured in the presence or absence of individual compounds was

Table 2: IC₅₀ values of anticancer activities of *Rheum emodi* Wall fractions on each cancer cell lines

Cell	Fraction	IC ₅₀ (µg/mL)
A549	n-Hexan	106.14 ± 4.42 ^c
	n-Butanol	103.96 ± 2.56 ^c
	Ethylacetate	128.52 ± 4.92 ^d
	Dichloromethane	93.58 ± 2.71 ^b
	Water	74.88 ± 2.25 ^a
MCF-7	Doxorubicin*	75.66 ± 2.88 ^a
	n-Hexan	116.34 ± 2.47 ^{bc}
	n-Butanol	124.24 ± 9.90 ^c
	Ethylacetate	139.36 ± 7.84 ^d
	Dichloromethane	114.72 ± 2.99 ^b
	Water	122.68 ± 6.25 ^{bc}
	Doxorubicin*	50.82 ± 1.56 ^a

Each value represents means ± SD
Values within a column for each parameter followed by different letters are significantly different (*P* < 0.05)

determined by Greiss reagent assay. The results revealed that individual compounds with concentration of 50, 100 and 200 µg/mL substantially inhibited the LPS-induced NO production in a dose dependent manner (Table 3). The NO inhibition activity from individual compounds varied from 40.6 to 51.3 µg/mL at 50 µg/mL and the myricetin (3) was found to have the highest NO inhibition activity, while at 100 µg/mL myricetin and its derivatives significantly inhibited the NO activity. Likewise, the highest NO inhibition activity was recorded by Myricetin 3-galloylrhamnoside (2) at 200 µg/mL concentration (Table 3).

IL-6 inhibition activity of individual compounds: The isolated compounds concentration inhibited LPS-induced IL-6 production linearly. In this regard, at 50 µg/mL of isolated compound treatments, mycetrin exhibited the strongest IL-6 inhibition activity; while myricetin 3-galloylrhamnoside (2) showed the most potent IL-6 inhibitory effect with 0.90 µg/mL at 100 µg/mL concentration compared with the 1.41 µg/mL of cells were viable after LPS induced stimulation for 24 h (Table 3). Moreover, higher concentration (200 µg/mL) of isolated compound strongly inhibited the IL-6 activity in macrophages. Among isolated compounds, myricetin (3), myricetin 3-galloylrhamnoside and unknown compound strongly inhibited the LPS induced IL-6 production (Table 3).

IL-1β inhibition activity of isolated compounds: The results showed that isolated compounds significantly inhibited LPS-induced IL-1β production in a concentration-dependent manner. Low concentration (50 µg/mL) of isolated compounds possess strong IL-1β inhibition activity potential and at this concentration Myricetin was most effective; while at 100 µg/mL concentration, 576.78 µg/mL of cells unknown viable after LPS induced stimulation for 24 h and among isolated compounds. Unknown compound strongly inhibited the LPS induced IL-1β production in macrophages. However, Myricetin 3-rhamnoside substantially reduced the cell viability of RAW 264.7 at 200 µg/mL (Table 3).

TNF-α inhibition activity of isolated compounds: The increase in isolated compounds concentration significantly inhibited LPS-induced TNF-α production in a linear pattern.

Table 3: Comparison of NO, IL-6, IL-1 β and TNF- α inhibition activities of isolated compounds from *R. emodi* on RAW 264.7 cells

Concentration ($\mu\text{g/mL}$)	Compounds	NO inhibition activity ($\mu\text{g/mL}$)	IL-6 inhibition activity ($\mu\text{g/mL}$)	IL-1 β inhibition activity (pg/mL)	TNF- α inhibition activity (pg/mL)
50	Myricetin 3-rhamnoside	51.32 \pm 1.95 ^c	1.40 \pm 0.03 ^b	256.70 \pm 7.08 ^b	553.44 \pm 77.02 ^a
	Myricetin 3-galloylrhamnoside	47.23 \pm 2.05 ^{bc}	1.41 \pm 0.02 ^b	361.43 \pm 7.51 ^d	657.38 \pm 79.45 ^c
	Myricetin	40.60 \pm 7.02 ^a	1.33 \pm 0.05 ^a	180.63 \pm 11.80 ^a	549.75 \pm 22.13 ^a
	Unknown	44.58 \pm 4.71 ^{ab}	1.37 \pm 0.03 ^{ab}	332.41 \pm 6.72 ^c	618.69 \pm 44.84 ^b
100	Myricetin 3-rhamnoside	21.04 \pm 2.80 ^a	1.03 \pm 0.14 ^b	76.79 \pm 0.89 ^c	540.90 \pm 57.84 ^b
	Myricetin 3-galloylrhamnoside	21.05 \pm 2.67 ^a	0.90 \pm 0.26 ^a	80.96 \pm 2.06 ^c	458.61 \pm 50.62 ^a
	Myricetin	23.53 \pm 2.10 ^a	1.00 \pm 0.21 ^b	67.14 \pm 10.63 ^b	510.33 \pm 12.54 ^{ab}
	Unknown	27.42 \pm 14.92 ^a	1.06 \pm 0.13 ^b	56.16 \pm 5.22 ^a	461.23 \pm 12.08 ^a
	LPS(+)*	67.42	1.41	577.00	577.00
200	Myricetin 3-rhamnoside	4.14 \pm 2.30 ^a	0.20 \pm 0.05 ^b	6.63 \pm 0.73 ^a	343.20 \pm 121.03 ^a
	Myricetin 3-galloylrhamnoside	2.70 \pm 0.10 ^a	0.11 \pm 0.05 ^a	30.45 \pm 1.93 ^c	296.72 \pm 109.71 ^a
	Myricetin	3.26 \pm 0.72 ^a	0.08 \pm 0.01 ^a	31.52 \pm 1.12 ^c	381.64 \pm 9.53 ^a
	Unknown	3.46 \pm 0.91 ^a	0.12 \pm 0.06 ^a	27.32 \pm 3.30 ^b	350.33 \pm 5.41 ^a

Each value represents means \pm SD (n=5)

^{a-d} Values within a fraction followed by different letters are significant different ($P < 0.05$)

* LPS(+): Values within a lipopolysaccharide stimulated macrophage RAW 264.7 cell

After treatment with 100 $\mu\text{g/mL}$ of the compounds, myricetin 3-galloylrhamnoside (2) exhibited the greatest potent TNF- α inhibitory effect with 458.61 pg/mL , compared with the 742.79 pg/mL of cells were viable after LPS induced stimulation for 24h. The myricetin 3-galloylrhamnoside (2) was found to have the highest IL-6 inhibition activity, with 296.71 pg/mL at high concentration (200 $\mu\text{g/mL}$) followed by: myricetin 3-rhamnoside (343.20 pg/mL) > unknown (350.33 pg/mL) > myricetin (381.64 pg/mL), (Table 3).

Anti-inflammatory activities of solvent extract fractions of *R. emodi*

NO inhibition activity of *R. emodi* solvent extract fractions on RAW 264.7 cells: The results showed that water and organic solvent fractions with various concentration (50, 100 and 200 $\mu\text{g/mL}$) significantly inhibited LPS-induced NO production in a concentration-dependent manner. At the concentration of 50 $\mu\text{g/mL}$, the NO inhibition activity from *R. emodi* fraction varied from 45.0 to 50.1 $\mu\text{g/mL}$. The ethyl acetate fraction (50 $\mu\text{g/mL}$) was found to have the highest NO inhibition activity (45.04 $\mu\text{g/mL}$); while Dichloromethane fraction at 200 $\mu\text{g/mL}$ exhibited the strongest NO inhibition activity (4.09 $\mu\text{g/mL}$) than rest of the fractions (Table 4).

IL-6 inhibition activity of *R. emodi* solvent extract fractions on RAW 264.7 cells: The IL-6 production was measured in the medium of RAW 264.7 cells cultured with LPS in the presence or absence of five fractions. The results showed that all the fractions significantly inhibited LPS-induced IL-6 production in a concentration-dependent manner. However, the response of each fraction varied greatly at different concentration. For instance, at 50 $\mu\text{g/mL}$ ethyl acetate fraction had the highest IL-6 inhibition activity. Likewise, ethyl acetate and n-Hexane fractions of *R. emodi* exhibited strong IL-6 inhibition activity at 100 $\mu\text{g/mL}$; while in dichloromethane fraction at 200 $\mu\text{g/mL}$ possessed

the strongest IL-6 inhibition activity (0.88 $\mu\text{g/mL}$) (Table 4). The water fraction exhibited the lowest IL-6 inhibition activity compared to all organic solvent fractions at all concentrations.

IL-1 β inhibition activity of *R. emodi* solvent extract fractions on RAW 264.7 cells: All the solvent extract *R. emodi* fractions significantly inhibited LPS-induced IL-1 β production in a concentration-dependent manner. The IL-1 β inhibition activity of *R. emodi* fraction varied from 159.5 to 201.3 pg/mL at low concentration (50 $\mu\text{g/mL}$). The ethyl acetate fraction was found to have the highest IL-1 β inhibition activity at 50 $\mu\text{g/mL}$; while n-Hexane fraction was most efficient in inhibiting the IL-1 β activity at 100 $\mu\text{g/mL}$. Nevertheless, at high concentration (200 $\mu\text{g/mL}$) *R. emodi* fractions progressively enhanced the IL-1 β inhibition activity and complete inhibition of IL-1 β activity in RAW 264.7 cells were observed with dichloromethane fraction (Table 4).

TNF- α inhibition activity of *R. emodi* solvent extract fractions on RAW 264.7 cells: The LPS-induced TNF- α production was significantly inhibited by all solvent extract fractions in a concentration-dependent manner. At low concentration (50 $\mu\text{g/mL}$) there was no significant difference among *R. emodi* fractions for TNF- α inhibition activity, while at 100 $\mu\text{g/mL}$ water fraction substantially enhanced the TNF- α inhibition activity. Moreover, at the concentration of 200 $\mu\text{g/mL}$, the n-butanol fraction was found to have the highest TNF- α inhibition activity (309.3 pg/mL) and possess the strongest anti-inflammatory activity among all other fractions (Table 4).

Classification pattern for isolated compounds and solvent extract fractions of *R. emodi* for their anti-inflammatory activities

The individual score showed its pattern, change and cluster formation that contained anti-inflammatory activities of compounds from *R. emodi*. Accordingly, as shown in Fig. 9,

Table 4: Comparison of NO, IL-6, IL-1 β and TNF- α inhibition activities of solvent extract fractions concentrations of *R. emodi* on RAW 264.7 cells

Concentration ($\mu\text{g/mL}$)	Fraction	NO inhibition activity ($\mu\text{g/mL}$)	IL-6 ($\mu\text{g/mL}$)	IL-1 β inhibition activity ($\mu\text{g/mL}$)	TNF- α inhibition activity ($\mu\text{g/mL}$)
50	n-Hexan	47.25 \pm 1.49 ^{ab}	8.04 \pm 2.32 ^b	189.58 \pm 6.54 ^a	692.54 \pm 49.94
	n-Butanol	50.12 \pm 1.34 ^b	9.19 \pm 1.71 ^{ab}	172.41 \pm 36.34 ^{ab}	643.52 \pm 31.90
	Ethylacetate	45.04 \pm 6.17 ^a	6.78 \pm 0.95 ^a	159.46 \pm 36.65 ^{ab}	656.48 \pm 105.87
	Dichloromethane	47.65 \pm 0.63 ^{ab}	9.07 \pm 0.87 ^{ab}	201.25 \pm 13.44 ^b	686.47 \pm 116.91
	Water	47.17 \pm 1.78 ^{ab}	11.66 \pm 1.97 ^c	198.39 \pm 7.17 ^b	699.92 \pm 161.45
100	n-Hexan	34.60 \pm 8.90	3.83 \pm 0.95 ^a	27.50 \pm 24.44 ^a	595.08 \pm 94.86 ^b
	n-Butanol	26.17 \pm 2.34	5.69 \pm 1.01 ^b	33.13 \pm 8.46 ^{ab}	579.18 \pm 46.09 ^{ab}
	Ethylacetate	26.66 \pm 15.4	3.80 \pm 0.85 ^a	39.46 \pm 14.05 ^{ab}	620.66 \pm 48.97 ^b
	Dichloromethane	29.65 \pm 1.00	4.99 \pm 0.71 ^{ab}	53.75 \pm 16.41 ^{bc}	560.25 \pm 41.26 ^{ab}
200	Water	30.27 \pm 1.18	8.35 \pm 1.10 ^c	65.80 \pm 11.67 ^c	514.92 \pm 20.87 ^a
	n-Hexan	7.56 \pm 1.49 ^b	2.84 \pm 0.47 ^c	4.64 \pm 1.03 ^c	468.61 \pm 71.58 ^b
	n-Butanol	6.38 \pm 1.00 ^b	2.53 \pm 0.53 ^c	5.27 \pm 1.74 ^c	309.34 \pm 52.58 ^a
	Ethylacetate	7.51 \pm 1.62 ^b	1.76 \pm 0.4 ^b	1.21 \pm 1.13 ^{ab}	469.59 \pm 59.31 ^b
	Dichloromethane	4.09 \pm 2.41 ^a	0.88 \pm 0.30 ^a	0 ^a	489.84 \pm 52.04 ^b
	Water	6.40 \pm 1.14 ^b	4.17 \pm 0.69 ^d	2.23 \pm 1.79 ^b	470.98 \pm 7.75 ^b

Each value represents means \pm SD

values within a column for each concentration followed by different letters are significantly different ($p < 0.05$)

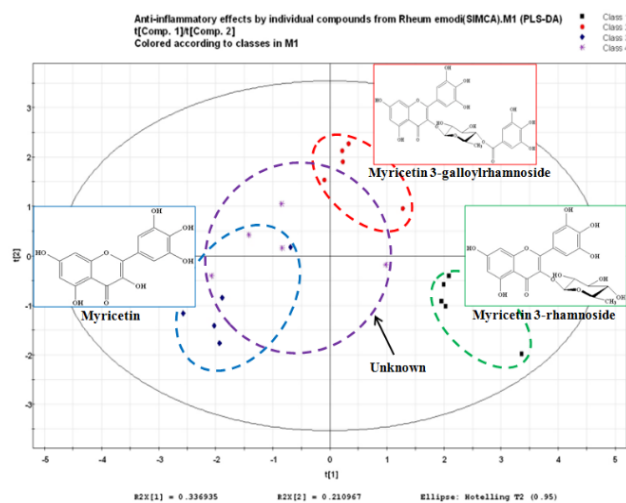


Fig. 9: Score plotting chart of principal component 1 and 2 of the PLS-DA results obtained from the data set by compounds profiling on the anti-inflammatory compounds. This chart showed classification by origin on all samples

(Green circle: Myricetin 3-rhamnoside, Purple circle: Unknown, Red circle: Myricetin- 3-galloylrhamnoside, Blue circle: Myricetin)

the correlation of anti-inflammatory activities and compounds (Myricetin 3-o-rhamnoside, Myricetin 3-galloylrhamnoside, Myricetin and unknown) were expressed through PLS-DA score plotting (Fig. 9). They could be grouped in four different groups. The compounds belong to left cluster than the ones on right cluster showed comparably higher anti-inflammatory activities. The cluster for blue color in compound (Myricetin) was located on the left side. The others make cluster for red color in Myricetin 3-galloylrhamnoside was located on the top-right side and green color in Myricetin 3-o-rhamnoside was located on the bottom (Fig. 9). As a result, anti-inflammatory

activities are related to the structure of compound and its contents, and it meant that the compound belong to myricetin cultivar had higher anti-inflammatory activities than the other compounds belong to Myricetin 3-o-rhamnoside, Myricetin 3-galloylrhamnoside and Unknown cultivars. Also, the Myricetin 3-galloylrhamnoside showed that the gallate acylation on the glycoside moiety on a flavonoid had higher anti-inflammatory activities than the Myricetin 3-o-rhamnoside; however, the potency did not exceed the activity of corresponding aglycon.

The correlation of anti-inflammatory activities and fractions (n-Hexan, n-Butanol, Ethyl acetate, Dichloromethane, and water) were expressed through PLS-DA score plotting. The fractions belong to right cluster (green and blue circle) showed comparably higher anti-inflammatory activity than the ones on left cluster (purple and red circle) showed comparably higher anti-inflammatory activities. Especially, it was confirmed that Water and n-Butanol belong to left cluster (yellow green), and Ethyl acetate and Dichloromethane belong to right cluster (yellow), but n-Hexane fraction was mixed up from other fractions (Fig. S4).

Discussion

The currently used all therapies for cancer treatment, particularly chemical synthesized drugs exhibit significant cytotoxicity to normal cells (Gupta *et al.* 2013). This study showed the potential of different fractions (organic and aqueous) of *R. emodi* rhizome extracts against anticancer and anti-inflammatory activities. In current study, the aqueous and organic solvent fractions of *R. emodi* exhibited strong anticancer activities. The aqueous and organic solvent extract fractions significantly ($P < 0.05$) enhanced the anticancer activities against A549 and MCF-7 cancer cell lines which can be attributed to the presence of compounds such as

anthraquinones, polyphenols (flavonoids), antra glycosides *etc.* in *R. emodi* fractions known for their antifungal, antibacterial and lipid homeostasis activities. Moreover, the activities of *R. emodi* fractions were strongly influenced by the solvent used. These differences in activities of different solvents can be ascribed to existence of distinctive protective metabolites extracted by the different solvents and solubility or stereoselectivity of the fractions (Yu *et al.* 2002).

Some naturally occurring flavonoids have exhibited selective toxicity to human cancer cells accompanied by very low toxicity to normal cells (Sak 2014). The positive effects of flavonoids in cancer treatment are associated to their strong antioxidant ability, including their capability to scavenge ROS. Several natural flavonoids targets caspases and therefore potent candidate as cancer chemotherapeutic agents (Raffa *et al.* 2017). One such flavonoid is myricetin (a dietary flavonoid) present in fruits, vegetables, medicinal plants including *R. emodi* (Fig. 1–5; Devi *et al.* 2015). Myricetin has been found to exert several antitumor roles in various types of cancers which include, antiproliferation, apoptosis induction and anti-metastatic activities (Iyer *et al.* 2015; Xu *et al.* 2015; Raffa *et al.* 2017) In present study, the isolated compounds (Myricetin and its derivatives) from *R. emodi* extracts efficiently inhibited the proliferation and induced the apoptosis in MCF-7 and A549 cancer cells (Table 1 and Fig. 7–8), which can be ascribed to the involvement of myricetin in upregulation of pro-apoptosis proteins and downregulation of ERK1/2 and AKT phosphorylation levels, Bcl-2 protein in cancer cell lines (Raffa *et al.* 2017; Park *et al.* 2020) and activation of caspase-3 in cancer cell lines (Raffa *et al.* 2017). The isolated compounds (myricetin 3-O-rhamnoside, myricetin 3-O-galloylrhamnoside, myricetin and unknown) in present study exhibited the anticancer activities in a dose dependent manner as higher concentration of myricetin exhibit the antiproliferative activities against cancer cells (Sun *et al.* 2012). Moreover, myricetin reduces the Matrix metalloproteinase 9 (MMP9) (member of MMP family of 24 zinc-dependent endopeptidases involved in induction of pro-IL-1 β cleavage and microglial activation) expression showing the antimetastatic effect (Raffa *et al.* 2017). The present study suggests that the isolated compounds from the *R. emodi* extract can be used as potential cancer therapeutics.

Inflammation is the key part of innate immunity and inflammatory response of a living tissue caused by noxious chemical stimuli, physical injury or infection (Wahab *et al.* 2018). The acute and chronic inflammation has been treated with different plant extracts in traditional medicine. Here, we observed that the aqueous and organic solvents extract fractions of *R. emodi* inhibited the LPS induced NO production in RAW 264.7 cells. The RAW 264.7 cells are macrophages used for evaluation of anti-inflammatory responses and drug screening (Lee *et al.* 2014). This inhibition of NO production in macrophage RAW 264.7 cells by *R. emodi*

fractions may be accredited to presence of flavonoids in these fractions (Table 4).

These plant extracts often have active constituent of flavonoids and related compounds, which possesses strong anticancer, antiinflammation, antiviral and immunomodulatory activities *etc.* (Russo *et al.* 2000; Havsteen 2002). The association of an aromatic ring to heterocyclic ring and functional group oxidation state of heterocyclic ring serves as the bases for flavonoids classification (Beecher 2003). The flavanols are the most abundant flavonoids; usually present in large quantities in vegetables and fruits in the form of aglycone or glycoside including myricetin, quercetin and kaempferol (Shukla *et al.* 2019). Myricetin (myricetin-3-glucoside, myricetin-3-rhamnoside) is an important bioflavonoid known for their anti-inflammatory activities (Table; Fig; Skrovankova *et al.* 2015). In Raw 264.7 macrophages, LPS induced pro-inflammatory mediators and cytokines play crucial role in inflammation induction. Nitric oxide (NO) is well known mediator and reacts with superoxide derived from macrophages in response to stimuli and produce cytotoxic peroxynitrite, which is involved in the inflammatory matrix metalloproteinase and cytokines production (Jarvinen *et al.* 2008). Further, the isolated Myricetin derivatives at higher doses attenuated the NO production (Table 2), which can be ascribed to role of these compounds in iNOS expression downregulation (Cho *et al.* 2016).

The pro-inflammatory cytokines such as IL-6, IL-1 β and TNF- α are well known, which are involved in inflammation induction. Bavia *et al.* (2015) revealed that LPS induced acute lung injury through increased production of IL-6, IL-1 β and TNF- α along with histopathological changes, alveolar wall thickening *etc.* which can be counteracted by bioactive compounds isolated from plants (Niu *et al.* 2014). In present study, *R. emodi* solvent extract fractions inhibited the IL-6, IL-1 β and TNF- α activity similar to NO in RAW 264.7 macrophage cells (Table 4). Here, all *R. emodi* fractions substantially inhibited the IL-6, IL-1 β and TNF- α activities in dose dependent manner. Ethyl acetate was more effective at lower concentration (50 and 100 $\mu\text{g/mL}$) for IL-6, IL-1 β inhibition activity; while dichloromethane was most effective fractions at higher dose (200 $\mu\text{g/mL}$) and even complete inhibition of IL-1 β activity was observed in RAW 264.7 macrophages. The differential response of these fractions may be due presence of different metabolites in these fractions and their solubility. Furthermore, the compounds (myricetin and its derivatives) isolated from the ethyl acetate fraction substantially inhibited the activities of pro-inflammatory cytokines (IL-6, IL-1 β and TNF- α) (Table 3); which can be attributed to Myricetin role in limiting NF- κB activity through subduing the I $\kappa\text{B}\alpha$ degradation, nuclear translocation of NF- κB (p65 subunit) and NF- κB DNA binding activity in LPS stimulated macrophages (RAW264.7) (Cho *et al.* 2016); as myricetin administration has been testified for inhibition of pro-inflammatory cytokines activities (Niu *et al.* 2014; Cho

et al. 2016). Furthermore, the higher antiinflammatory activities of isolated compounds are due to myricetin involvement in HO-1 expression induction via Nrf2 translocation. The isolated compounds (myricetin, myricetin-3-O-galactoside and myricetin-3-O-rhamnoside) from ethyl acetate fraction of *R. emodi* indicate that these compounds can be used for treatment of inflammation disorders.

PLS-DA is much more advantageous to distinguish the characteristics of pre-defined groups compared to the existing PCA (Perez-Enciso and Tenenhaus 2003). PLS-DA is discriminating the assigned cluster characteristics. It is variance that affects the cluster formation or considered as important of compound information. Metabolite analysis data can be visualized through range; standardization and major component score (Cho 2013). The Galloyl flavanol glycosides protect macrophages from the inflammatory response through the limiting the expression of COX-2. The Galloyl group showed enhanced COX-2 expression than their parent compounds (Kim *et al.* 2004). Although this discrepancy in the results cannot fully be explained at this stage, it may come from different assay system used or, possibly, to the different attachment position of the galloyl group. It can be recognized as the promising flavonoid anti-inflammatory with *R. emodi* being a good source of the flavonoids.

Conclusion

The result of present study showed the potential of aqueous and organic solvent *R. emodi* rhizome fractions and isolated flavonoids for anti-cancer and anti-inflammatory activities. The Flavonoids (myricetins) isolated and identified from ethyl acetate fraction of *R. emodi* exhibited strong cytotoxicity and anti-inflammatory activities on cancer cell lines (MCF-7 and A549) and LPS stimulated macrophages (RAW 264.7), respectively. The higher concentration ($\leq 100 \mu\text{M}$) aqueous/organic fractions and isolated compounds strongly inhibited the LPS stimulated TNF- α , IL-6 and IL-1 β and NO production in macrophages and induced the apoptosis and restricted the proliferation in cancer cell lines. However, myricetin and unknown compounds were most effective at lower concentration (50 $\mu\text{g/mL}$) for anti-inflammatory and anticancer response, suggesting that the isolated compounds can be used for drug development for cancer and inflammation treatment.

Author Contributions

Sang KP and SY Im conceived the idea, Sang KP conducted the study, SY Im analyzed the data and prepared the manuscript draft for submission

Conflict of Interest

The authors declare no conflict of interests

Data Availability

The data supporting the findings of this study are available within the article and its supplementary materials.

Ehics Approval

All procedures performed in this study involving human or animal cells were in accordance with the ethical standards of the institution at which the studies were conducted

References

- Amani T, I Iswaldi, D Arráez-Román, A Segura-Carretero, A Fernández-Gutiérrez, M Zarrouk (2014) UPLC-QTOF/MS for a rapid characterisation of phenolic compounds from leaves of *Myrtus communis* L. *Phytochem Anal* 25:89–96
- Bavia L, IAD Castro, L Isaac (2015). C57BL/6 and A/J mice have different inflammatory response and liver lipid profile in experimental alcoholic liver disease. *Mediat Inflamm* 2015; Article 491641
- Beecher GR (2003). Overview of dietary flavonoids: Nomenclature, occurrence and intake. *J Nutr* 133:3248–3254
- Cho BO, HH Yin, SH Park, EB Byun, HY Ha, SI Jang (2016). Anti-inflammatory activity of myricetin from *Diospyros lotus* through suppression of NF- κ B and STAT1 activation and Nrf2-mediated HO-1 induction in lipopolysaccharide-stimulated RAW264. 7 macrophages. *Biosci Biotechnol Biochem* 80:1520–1530
- Cho YH (2013). Gamma (γ)-oryzanol compositions and functional activities in rice genetic resources. *Ph.D. Thesis*. Chungnam National University, Korea
- Choi J, NL Corder, B Koduru, Y Wang (2014). Oxidative stress and hepatic Nox proteins in chronic hepatitis C and hepatocellular carcinoma. *Free Rad Biol Med* 72:267–284
- Choi WS, PG Shin, JH Lee, GD Kim (2012). The regulatory effect of veratric acid on NO production in LPS-stimulated RAW264.7 macrophage cells. *Cell Immunol* 280:164–170
- Cragg GM, DJ Newman (2007). Plants as a source of anti-cancer agents. *J Ethnopharmacol* 100:72–79
- Devi KP, T Rajavel, S Habtemariam, SF Nabavi, SM Nabavi (2015). Molecular mechanisms underlying anticancer effects of myricetin. *Life Sci* 142:19–25
- Gao LL, XD Xu, HJ Nang, JS Yang, SL Chen (2011). Chemical Constituents in *Rheum tanguticum*. *Chin Trad Herb Drugs* 42:443–446
- Gupta A, BS Kumar, AS Negi (2013). Current status on development of steroids as anticancer agents. *J Ster Biochem Mol Biol* 137:242–270
- Havsteen B (2002). The biochemistry and medical significance of the flavonoids. *Pharmacol Ther* 96:67–202
- Iqbal J, BH Abbasi, T Mahmood, S Kanwal, B Ali, SA Shah, AT Khalil (2017). Plant-derived anticancer agents: A green anticancer approach. *Asian Pac J Trop Biomed* 7:1129–1150
- Iyer SC, A Gopal, D Halagowder (2015). Myricetin induces apoptosis by inhibiting P21 activated kinase 1 (PAK1) signaling cascade in hepatocellular carcinoma. *Mol Cell Biochem* 407:223–237
- Jarvinen K, K Vuolteenaho, R Nieminen, T Moilanen, RG Knowles, E Moilanen (2008). Selective iNOS inhibitor 1400 W enhances anti-catabolic IL-10 and reduces destructive MMP-10 in OA cartilage. Survey of the effects of 1400W on inflammatory mediators produced by OA cartilage as detected by protein antibody array. *Clin Exp Rheumatol* 26:275–282
- Kim HK, GM NA, SU Ye, HS Han (2004). Extraction characteristics and antioxidative activity of *Schizandra chinensis* extracts. *Kor J Food Cult* 19:484–490
- Kounsar F, ZM Afzal (2010). *Rheum emodi* induces nitric oxide synthase activity in murine macrophages. *Amer J Biomed Sci* 2:155–162
- Krishnamurthi K (2007). 17-screening of natural products for anticancer and antidiabetic properties. *Cancer* 3:69–75

- Lee J, K Sowndhararajan, M Kim, J Kim, D Kim, S Kim, GY Kim, S Kim, JW Jhoo (2014). Antioxidant, inhibition of α -glucosidase and suppression of nitric oxide production in LPS-induced murine macrophages by different fractions of *Actinidia arguta* stem. *Saud J Biol Sci* 21:532–538
- Li F, SC Wang, X Wang, QY Ren, W Wang, GW Shang, L Zhang, SH Zhang (2008). Novel exploration of cathartic pharmacology induced by rhubarb. *Chin J Chin Mater Med* 33:481–484
- Li YC, YF Xian, ZR Su, SP Ip, JH Xie, JB Liao, DW Wu, CW Li, JN Chen, ZX Lin, XP Lai (2014). Pogostone suppresses proinflammatory mediator production and protects against endotoxic shock in mice. *J Ethnopharmacol* 157:212–221
- Lin LZ, JA Harnly (2007). Screening method for the identification of glycosylated flavonoids and other phenolic compounds using a standard analytical approach for all plant materials. *J Agric Food Chem* 55:1084–1096
- Niu N, B Li, Y Hu, X Li, J Li, H Zhang (2014). Protective effects of scoparone against lipopolysaccharide-induced acute lung injury. *Intl Immunopharmacol* 23:127–133
- Park S, G Song, W Lim (2020). Myricetin inhibits endometriosis growth through cyclin E1 down-regulation *in vitro* and *in vivo*. *J Nutr Biochem* 78:108328
- Pereira SS, JI Alvarez-Leite (2014). Low-grade inflammation, obesity, and diabetes. *Curr Obes Rep* 3:422–431
- Perez-Enciso M, M Tenenhaus (2003). Prediction of clinical outcome with microarray data: A partial least squares discriminant analysis (PLS-DA) approach. *Hum Genet* 112:581–592
- Qian BZ (2017). Inflammation fires up cancer metastasis. In: *Seminars in Cancer Biology*, Vol. 47, pp:170–176. Academic Press, London, UK
- Raffa D, B Maggio, MV Raimondi, F Plescia, G Daidone (2017). Recent discoveries of anticancer flavonoids. *Eur J Med Chem* 142:213–228
- Rajkumar V, G Guha, RA Kumar (2011). Apoptosis Induction in MDA-MB-435S, Hep3B and PC-3 Cell Lines by *Rheum emodi* rhizome extracts. *Asian Pac J Cancer Prevent* 12:1197–1200
- Rokaya MB, Z Münzbergová, B Timsina, KR Bhattarai (2012). *Rheum australe* D. Don: A review of its botany, ethnobotany, phytochemistry and pharmacology. *J Ethnopharmacol* 141:761–774
- Russo A, R Acquativiva, A Campisi, V Sorrenti, CD Giacomo, G Virgata (2000). Bioflavonoids as antiradicals, antioxidants and DNA cleavage protectors. *Cell Biol Toxicol* 16:91–96
- Sak K (2014). Site-specific anticancer effects of dietary flavonoid quercetin. *Nutr Cancer* 66:177–193
- Shukla R, V Pandey, GP Vadnere, S Lodhi (2019). Role of flavonoids in management of inflammatory disorders. In: *Bioactive Food as Dietary Interventions for Arthritis and Related Inflammatory Diseases*, pp:293–322. Academic Press, London, UK
- Skrovankova S, D Sumczynski, J Mlcek, T Jurikova, J Sochor (2015). Bioactive compounds and antioxidant activity in different types of berries. *Intl J Mol Sci* 16:24673–24706
- Sun F, XY Zheng, J Ye, TT Wu, JL Wang, W Chen (2012). Potential anticancer activity of myricetin in human T24 bladder cancer cells both *in vitro* and *in vivo*. *Nutr Cancer* 64:599–606
- Torres-Rodríguez ML, E García-Chávez, M Berhow, EGD Mejia (2016). Anti-inflammatory and anti-oxidant effect of *Calea urticifolia* lyophilized aqueous extract on lipopolysaccharide-stimulated RAW 264.7 macrophages. *J Ethnopharmacol* 188:266–274
- Wahab ASM, I Jantan, M Haque, L Arshad (2018). Exploring the leaves of *Annona muricata* L. as a source of potential anti-inflammatory and anticancer agents. *Front Pharmacol* 9: Article 661
- Xu YC, SWS Leung, GPH Leung, RYK Man (2015). Kaempferol enhances endothelium-dependent relaxation in the porcine coronary artery through activation of large-conductance Ca^{2+} -activated K^{+} channels. *British J Pharmacol* 172:3003–3014
- Yu L, S Haley, J Perret, M Harris, J Wilson, M Qian (2002). Free radical scavenging properties of wheat extracts. *J Agric Food Chem* 50:1619–1624